IOP Conf. Series: Journal of Physics: Conf. Series **842** (2017) 012061 doi:10.1088/1742-6596/842/1/012061

# Numerical Simulation of cracked orthotropic materials using extended isogeometric analysis

**S H Habib[1], I Belaidi[1], S Khatir[2] and M Abdel Wahab[2]**

[1] Department of Mechanical Engineering, University of M'hamed Bougara, Boumerdes, Algeria

[2] Department of Electrical Energy, Systems and Automation, Faculty of Engineering and Architecture, Ghent University, Belgium

Email: magd.abdelwahab@ugent.be

**Abstract**. In the present study, extended isogeometric analysis (XIGA) is used to analyse cracks in orthotropic media. NURBS and T-splines geometric technologies are used to define the geometry and the solution. Knot insertion and order elevation are used in NURBS models, while a new local refinement algorithm is applied to T-spline models. In XIGA, the basic idea of the extended finite element method (X-FEM) is used along with isogeometric analysis for modelling discontinuities by including enrichment functions. Special orthotropic crack tip enrichments are used to reproduce the singular fields near a crack tip, and fracture properties of the models are defined by the mixed mode stress intensity factors (SIFs), which are obtained by means of the interaction integral (M-integral). Results of the proposed method are compared with other available results.

## 1. Introduction

Composite materials are not immune to manufacture defects such as voids, inclusions and cracks. The crack problems greatly influence in the macroscopic response of composites materials, and this lead to the need for better understanding and analyzing the behavior of these materials under applied loads especially in critical conditions.

Analytical studies based upon the laws of fracture mechanics of composites are available [1-5]. However, the complexity of the analytical solutions even for simple cases requires modelling the mechanical behaviour of this problem using effective numerical methods. Among them we distinguish, boundary element method (BEM) [6], finite element method (FEM) [7-14], which has wide range of applications [8, 11, 15-21], element free Galerkin method (EFGM) [22], extended finite element method (XFEM) [23] and other methods [24, 25]. A few years ago, isogeometric analysis was introduced by Hughes et *al*. [26] as an alternative to other methods. This method is based on the idea of using the same functions adopted in Computer Aided Design (CAD) not only to describe the domain geometry, but also to build the numerical approximation of the problem solution [27-35]. It has been developed and applied in many fields, such as: structural vibrations [33-40], with applications to structural health monitoring (SHM) [41-46], contact problems [47], piezoelectric [33, 34, 38] materials [48], blood flow [49], electromagnetics [50], shape optimization [51] and fracture mechanics [52]. However in fracture mechanics problems, IGA faces certain difficulties that are already exist in finite element method (FEM). This makes IGA a suitable candidate to be extended in the same way that FEM improved.

Recently, IGA was enhanced using the partition unity enrichment, but with local enrichment functions in order to capture the discontinuous without any explicit meshing, this method is known as extended isogeometric analysis (XIGA). For fracture mechanics, XIGA is characterized by the accuracy and the high convergence rate in such problems, as shown in [53]. Many investigations were performed using XIGA, such as in fatigue crack growth [54], thin shell analysis, Helmholtz problems, piezoelectric materials and composite materials [55-61].

The most widely geometric function used in CAD is the NURBS, due to its simplicity and its efficiency in geometrical representations, especially all conical sections, which can be represented exactly, such as, circles, cylinders, spheres and ellipsoids. NURBS basis functions have very useful mathematical properties, like partition of unity, compact support, and high degree of continuity. Also, NURBS are characterized by the multitude of refinement methods (*h*-refinement, *p*-refinement, *k*-refinement). In addition, there are many effective algorithms that can be programmed numerically to generate NURBS objects. As in CAD, NURBS was also used for IGA in most researches, because their mathematical properties are always compatible with analysis conditions regardless of the used geometric shape. Despite all the advantages mentioned there are some disadvantages observed during the analysis, which cannot be avoided even by using multiple patches, where NURBS generates a complicated mesh, which lead to produce superfluous control points.

Sederberg *et al.* [62] proposed T-splines as more generalized tools than NURBS in order to handle their disadvantages. T-splines are characterized by their robustness in the generation of adjacent patches, and also by the local refinement property of the mesh even for a single patch. In addition, T-splines provide several algorithms that can be used to refine geometries locally. Recently, T-splines were introduced as additional modules in some CAD software, like Maya and Rhino. As part of the IGA, T-splines are considered as applicable analytical tools that have proven to be efficient in several studies. From the analysis point of view, T-splines allow to use a minimum number of degrees of freedom compared to the number that can be used in the NURBS, and this leads to simplify the computation. In some domains, T-splines are considered as a better tool for IGA, like in the fracture mechanics, contact mechanics and mechanics of bi-materials, generally in any domain where the property of local refinement is necessary and the geometry is complex. However T-spline bases are not always valid to be used in analysis for different geometric configurations, because the linear independent and the partition unity properties are not always ensured. Li et al. [63] introduced analysis-suitable T-spline, where for any choice of knot vectors the blending functions are linearly independent. Like NURBS bases, analysis-suitable T-spline bases have the properties of the analysis basis functions. Moreover, they provide an efficient algorithm, which allows making highly localized refinement [64].

In this paper, cracks in orthotropic media are analysed using XIGA, whereas NURBS and T-splines are used for modelling the crack and construct the geometry. Orthotropic crack tip enrichment functions [65-67] are implemented to accurately calculate the displacement and stress fields, and mixed mode stress intensity factors (SIFs) are numerically evaluated using the interaction integral (M-integral) [68] to determine fracture properties of the domain. An edge and central crack are investigated by considering the effect of fibre orientation.

## 2. Fracture mechanics for 2D orthotropic materials

Consider a cracked elastic homogeneous orthotropic body $\Omega$ subjected to traction forces $f_t$ applied at $\Gamma_t$ and displacement conditions applied at $\Gamma_u$ in the absence of body forces, as shown in Figure 1. The partial differential equation of the stress functions of this problem can be obtained using equilibrium and compatibility conditions [69]:

$$c_{22}\frac{\partial^4\varphi}{\partial x^4}-2c_{26}\frac{\partial^4\varphi}{\partial x^3\partial y}+\left(2c_{12}+c_{66}\right)\frac{\partial^4\varphi}{\partial x^2\partial y^2}-2c_{16}\frac{\partial^4\varphi}{\partial x\,\partial y^3}+c_{11}\frac{\partial^4\varphi}{\partial y^4}=0 \tag{1}$$

where $(x,y)$ is local Cartesian coordinates, $\varphi$ is the stress function and $c_{ij}$ is the components of the compliance matrix, which is computed in terms of Young moduli ($E_1$, $E_2$), Poisson ratios ($\nu_{12}$,$\nu_{13}$ and $\nu_{23}$) and shear modulus ($\mu_{12}$, $\mu_{13}$ and $\mu_{23}$) as follows:

$$c=\begin{bmatrix} 1/E_1 & -\nu_{12}/E_1 & -\nu_{13}/E_1 & 0 & 0 & 0 \\ -\nu_{12}/E_1 & 1/E_2 & -\nu_{23}/E_2 & 0 & 0 & 0 \\ -\nu_{13}/E_1 & -\nu_{23}/E_2 & 1/E_3 & 0 & 0 & 0 \\ 0 & 0 & 0 & 1/\mu_{23} & 0 & 0 \\ 0 & 0 & 0 & 0 & 1/\mu_{13} & 0 \\ 0 & 0 & 0 & 0 & 0 & 1/\mu_{12} \end{bmatrix} \tag{2}$$

The general characteristic equation of the partial differential equation is:

$$c_{11}s^4-2c_{16}s^3+\left(2c_{12}+c_{66}\right)s^2-2c_{26}s+c_{22}=0 \tag{3}$$

The four roots of this characteristic equation are complex and conjugated two-two ($s_1$, $\bar{s}_1$ and $s_2$, $\bar{s}_2$). These roots were used by [1] to derive the displacement and the stress fields in the vicinity of the crack tip for an infinite domain. The stress components for pure mode I are:

$$\begin{aligned} \sigma_{xx}^{I} &= \frac{K_I}{\sqrt{2\pi r}}Re\left[\frac{s_1 s_2}{s_1-s_2}\left(\frac{s_2}{\left(\cos\theta+s_2\sin\theta\right)^{1/2}}-\frac{s_1}{\left(\cos\theta+s_1\sin\theta\right)^{1/2}}\right)\right] \\ \sigma_{yy}^{I} &= \frac{K_I}{\sqrt{2\pi r}}Re\left[\frac{1}{s_1-s_2}\left(\frac{s_1}{\left(\cos\theta+s_2\sin\theta\right)^{1/2}}-\frac{s_2}{\left(\cos\theta+s_1\sin\theta\right)^{1/2}}\right)\right] \\ \sigma_{xy}^{I} &= \frac{K_I}{\sqrt{2\pi r}}Re\left[\frac{s_1 s_2}{s_1-s_2}\left(\frac{1}{\left(\cos\theta+s_1\sin\theta\right)^{1/2}}-\frac{1}{\left(\cos\theta+s_2\sin\theta\right)^{1/2}}\right)\right] \end{aligned} \tag{4}$$

and for pure mode-II:

$$\begin{aligned} \sigma_{xx}^{II} &= \frac{K_{II}}{\sqrt{2\pi r}}Re\left[\frac{1}{s_1-s_2}\left(\frac{s_2^{\,2}}{\left(\cos\theta+s_2\sin\theta\right)^{1/2}}-\frac{s_1^{\,2}}{\left(\cos\theta+s_1\sin\theta\right)^{1/2}}\right)\right] \\ \sigma_{yy}^{II} &= \frac{K_{II}}{\sqrt{2\pi r}}Re\left[\frac{1}{s_1-s_2}\left(\frac{1}{\left(\cos\theta+s_2\sin\theta\right)^{1/2}}-\frac{1}{\left(\cos\theta+s_1\sin\theta\right)^{1/2}}\right)\right] \\ \sigma_{xy}^{II} &= \frac{K_{II}}{\sqrt{2\pi r}}Re\left[\frac{1}{s_1-s_2}\left(\frac{s_1}{\left(\cos\theta+s_1\sin\theta\right)^{1/2}}-\frac{s_2}{\left(\cos\theta+s_2\sin\theta\right)^{1/2}}\right)\right] \end{aligned} \tag{5}$$

The displacements for pure mode-I are

$$\begin{aligned} u_x^I &= K_I\sqrt{\frac{2r}{\pi}}Re\left\{\frac{1}{s_1-s_2}\left[s_1 d_2\left(\cos\theta+s_2\sin\theta\right)^{1/2}-s_2 d_1\left(\cos\theta+s_1\sin\theta\right)^{1/2}\right]\right\} \\ u_y^I &= K_I\sqrt{\frac{2r}{\pi}}Re\left\{\frac{1}{s_1-s_2}\left[s_1 e_2\left(\cos\theta+s_2\sin\theta\right)^{1/2}-s_2 e_1\left(\cos\theta+s_1\sin\theta\right)^{1/2}\right]\right\} \end{aligned} \tag{6}$$

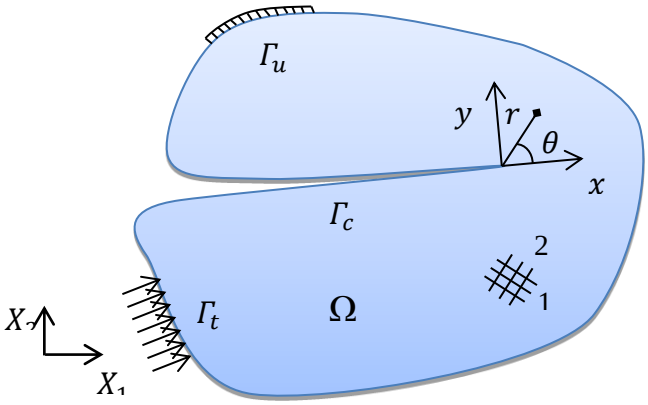


**Figure 1.** An arbitrary orthotropic cracked body with boundary conditions.

and for pure mode-II:

$$u_x^{II} = K_{II}\sqrt{\frac{2r}{\pi}}Re\left\{\frac{1}{s_1-s_2}\left[d_2\left(\cos\theta+s_2\sin\theta\right)^{1/2}-d_1\left(\cos\theta+s_1\sin\theta\right)^{1/2}\right]\right\}$$
$$u_y^{II} = K_{II}\sqrt{\frac{2r}{\pi}}Re\left\{\frac{1}{s_1-s_2}\left[e_2\left(\cos\theta+s_2\sin\theta\right)^{1/2}-e_1\left(\cos\theta+s_1\sin\theta\right)^{1/2}\right]\right\} \quad (7)$$

where *Re* represents the real part of a complex number, $K_I$ and $K_{II}$ are the stress intensity factors for modes I and mode II, respectively, and the constant values $d_i$ and $e_i$ are computed as:

$$d_i = c_{11}s_i^2 + c_{12} - c_{16}s_i \quad i = 1,2 \quad (8)$$

$$e_i = c_{12}s_i + \frac{c_{22}}{s_i} - c_{26} \quad i = 1,2 \quad (9)$$

The relation between energy release rate *G* and stress intensity factors was expressed by Sih et al. [1] for homogeneous composites as follows:

$$G_I = -\frac{\pi}{2}K_I c_{22}\,\mathrm{Im}\left[\frac{K_I(s_1+s_2)+K_{II}}{s_1 s_2}\right] \quad (10)$$

$$G_{II} = -\frac{\pi}{2}K_{II}c_{11}\,\mathrm{Im}\left[K_I(s_1+s_2)+K_{II}s_1s_2\right] \quad (11)$$

## 3. Non uniform rational B-splines (NURBS)

NURBS entities are constructed by linear combination of NURBS basis functions and their control points. NURBS bases are defined by one knot vector in each parametric direction. Univariate NURBS basis functions $R_i$ of order *p* are defined by:

$$R_{i,p}(\xi) = \frac{N_{i,p}(\xi)w_i}{\sum_{\hat{i}=1}^{n} N_{\hat{i},p}(\xi)w_{\hat{i}}} \quad (12)$$

where *n* is the number of basis functions, *w* is a set of positive weights, $\xi$ is a parametric coordinate of the first direction and $N_i$ are the B-spline basis functions corresponding to the knot vector $\Xi=\{\xi_1,\xi_2,.....,\xi_{n+p+1}\}$, they are given by:

$$N_{i,0}(\xi) = \begin{cases} 1 & \text{if } \xi_i \le \xi < \xi_{n+p+1} \\ 0 & \text{otherwise} \end{cases}, \quad \text{for } p = 0 \quad (13)$$

and

$$N_{i,p}(\xi)=\frac{\xi-\xi_i}{\xi_{i+p}-\xi_i}N_{i,p-1}(\xi)+\frac{\xi_{i+p+1}-\xi}{\xi_{i+p+1}-\xi_{i+1}}N_{i+1,p-1}(\xi);\quad \text{for } p>0 \tag{14}$$

For the two parametric directions $\xi$ and $\eta$, bivariate NURBS basis functions are given by:

$$R_{i,j}^{p,q}(\xi,\eta)=\frac{N_{i,p}(\xi)M_{j,q}(\eta)w}{\sum_{\hat{i}=1}^{n}\sum_{\hat{j}=1}^{m}N_{\hat{i},p}(\xi)M_{\hat{j},q}(\eta)w} \tag{15}$$

where $M_j$ are B-spline basis functions of order $q$ corresponding to the second knot vector H={$\eta_1,\eta_2,.....,\eta_{m+q+1}$} of which $m$ is the number of basis functions.

## 4. T-splines

In order to construct a T-spline surface, the T-mesh, which is a mesh of rectangular elements defined by the lines corresponding to knot values, as shown in Figure 2, must be defined according to the basis function orders $p$ and $q$ to extract the local knot vectors $\Xi_\alpha$ and $H_\alpha$, and compute the blending functions $\mathbf{R}_\alpha$ for each anchor. Then, in a similar way as for NURBS, we can define the T-spline surface by:

$$S=\sum_{\alpha=1}^{k}\mathbf{R}_\alpha \mathrm{P}_\alpha \tag{16}$$

where the blending functions given by:

$$\mathbf{R}_\alpha(\xi,\eta)=\frac{w_\alpha \mathbf{B}_\alpha(\xi,\eta)}{\sum_{\beta=1}^{k}w_\beta \mathbf{B}_\beta(\xi,\eta)} \tag{17}$$

and P is the control points, $\alpha$ is the anchor index, $k$ is the number of the anchors in T-mesh and **B** is the bivariate local basis function, which is given by:

$$\mathbf{B}_\alpha=N_{i,p}(\xi)M_{j,q}(\eta) \tag{18}$$

The refinement in T-splines is based on the subdivision of basis functions by insert knots to local knot vector. For one inserted knot $z$, there are two produced basis functions that are combined linearly to form the original basis function as:

$$N(\xi|\xi_1,...,\xi_5)=XN(\xi|\xi_1,...,\xi_4)+YN(\xi|\xi_2,...,\xi_5) \tag{19}$$

where

$$X=\begin{cases}\dfrac{z-\xi_1}{\xi_4-\xi_1} & \text{for } z<\xi_4\\ 1 & \text{for } z\geq\xi_4\end{cases} \tag{20}$$

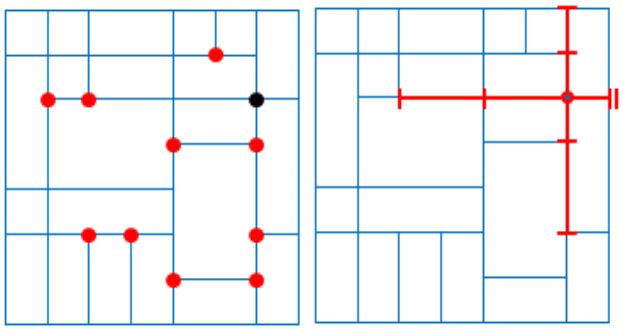

(a) (b)

**Figure 2.** Shows a T-mesh with: (a) T-junction points (red points) and (b) local support of black point.

$$Y = \begin{cases} \dfrac{\xi_5 - \mathrm{z}}{\xi_5 - \xi_2} & \text{for } \mathrm{z} > \xi_2 \\ 1 & \text{for } \mathrm{z} \le \xi_2 \end{cases} \tag{21}$$

For more than one inserted knot, the application of these equations is repeated until all coefficients are derived. In refined T-spline space, the relation between the original basis functions $\mathbf{B}^1$ and the generated basis functions $\mathbf{B}^2$ can be expressed in linear system form using the refinement operator $\mathbf{M}$

$$\mathbf{N}_1 = \mathbf{M}\mathbf{N}_2 \tag{22}$$

where $\mathbf{N}_1$ and $\mathbf{N}_2$ are the column vectors of blending functions of the original and the refined T-spline spaces, respectively.

## 5. Extended isogeometric analysis (XIGA)

In XIGA, the displacement approximation for cracks at a particular point $\zeta=(\xi,\eta)$, can be written in generalized form by extending the IGA approximation:

$$\mathrm{u}(\zeta) = \sum_{i=1}^{n_s} \boldsymbol{Q}_i(\zeta)\,\mathrm{u}_i + \sum_{j=1}^{n_{cf}} \boldsymbol{Q}_j(\zeta) H(\zeta) \mathrm{a}_j + \sum_{k=1}^{n_{ct}} \boldsymbol{Q}_k(\zeta) \left( \sum_{\ell=1}^{4} F_\ell(\zeta) \mathrm{b}_k^\ell \right) \tag{23}$$

where $\boldsymbol{Q}$ is the T-spline basis function ($\mathbf{R}$), Eq. 17 or NURBS basis function ($R$) Eq. 15. $H$ is the Heaviside function used for modelling the crack face, it takes the value 1 above the crack and -1 below the crack, $F$ are the crack-tip enrichment functions derived from the analytical solution of the displacement field around the crack tip, $u_i$, $a_j$ and $b_k$ are the displacement vectors correspond to $n_s$, $n_{cf}$ and $n_{ct}$ control points, respectively.

The crack-tip enrichment functions are obtained from the analytical solution of the displacement field in the vicinity of the crack-tip as [66]

$$\{F_\ell(r,\theta)\}_{\ell=1}^{4} = \left\{ \begin{matrix} \sqrt{r}\cos\left(\dfrac{\theta_1}{2}\right)\sqrt{g_1(\theta)}, \sqrt{r}\cos\left(\dfrac{\theta_2}{2}\right)\sqrt{g_2(\theta)} \\ \sqrt{r}\sin\left(\dfrac{\theta_1}{2}\right)\sqrt{g_1(\theta)}, \sqrt{r}\sin\left(\dfrac{\theta_2}{2}\right)\sqrt{g_2(\theta)} \end{matrix} \right\} \tag{24}$$

where $g_k(\theta)$ and $\theta_k$ are given by

$$g_k(\theta) = \sqrt{(\cos\theta + s_{kx})^2 + (s_{ky}\sin\theta)^2}; \quad \theta_k = \arctan\left( \frac{s_{ky}\sin\theta}{\cos\theta + s_{kx}\sin\theta} \right); \quad k = 1,2 \tag{25}$$

## 6. Numerical simulations

In this section, a circular orthotropic plate with a central crack and a rectangular orthotropic plate with an edge crack are simulated in the plane stress state. The corresponding boundary conditions are shown in Figure 3. First, in the circular plate ($E_1$=0.1 *GPa*, $E_2$=1 *GPa*, $\mu_{12}$=0.5 *GPa*, $\nu_{12}$=0.03) different inclined cracks are examined, where the orthotropic axes (1,2) coincide with the Cartesian axes ($x,y$). The problem is analysed using 793 control points and 688 elements (Figure 4). Variation of mode I and II SIF is presented in Figure 6. The obtained values in the case $\beta$=30° are compared with other values taken from the literature, as shown in Table 1. In the second part, several orientations of material elastic axes namely, $\gamma$=0°, 30°, 45°, 60° and 90° are investigated for the rectangular plate, which is composed of graphite-epoxy material ($E_1$=114.8 *GPa*, $E_2$=11.7 *GPa*, $\mu_{12}$=9.66 *GPa*, $\nu_{12}$=0.21). The T-spline mesh (1372 DOF) is constructed using 566 control points and 431 elements (Figure 5), and the NURBS mesh (3248 DOF) is constructed using 1624 control points and 1375 elements (Figure 5). The obtained normalized stress intensity factors $(\bar{K} = K / (\sigma\sqrt{\pi a}))$ are compared with those of the XFEM, as depicted in Figure 7.

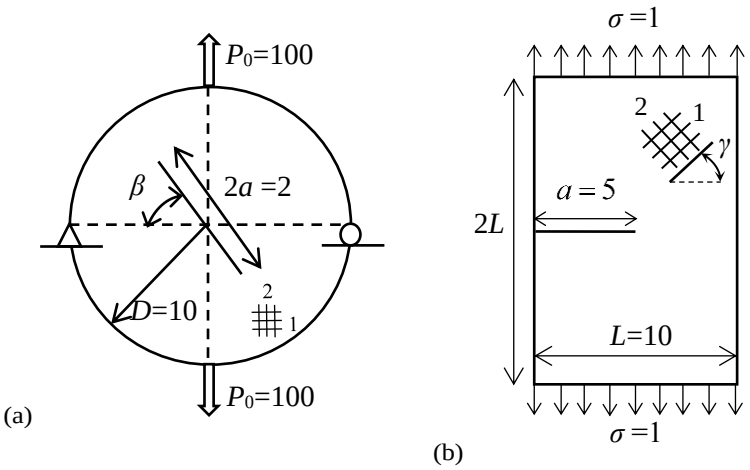


**Figure 3.** Geometries and boundary conditions for the homogeneous orthotropic examples: (a) a disk with a center crack and (b) a rectangular plate with an edge crack.

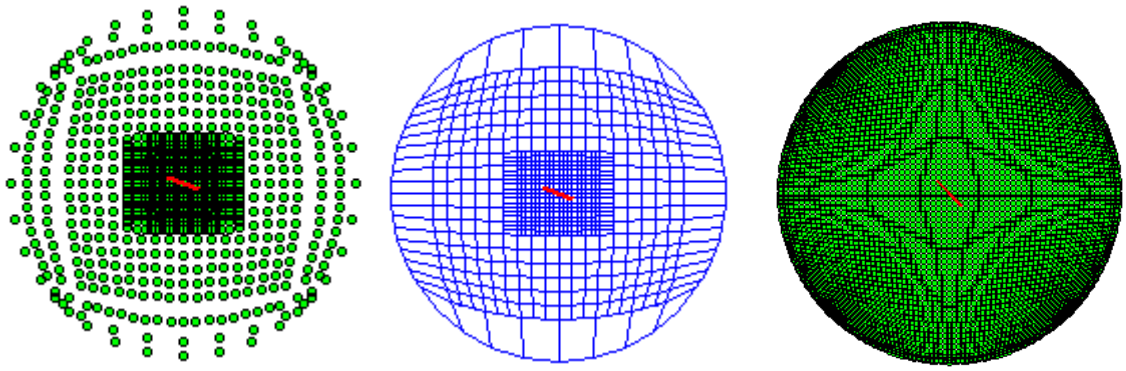


**Figure 4.** The meshes used for the circular plate example: (a) T-spline control net (793 points), (b) T-spline mesh (688 elements) et (c) NURBS control net (4489 points).

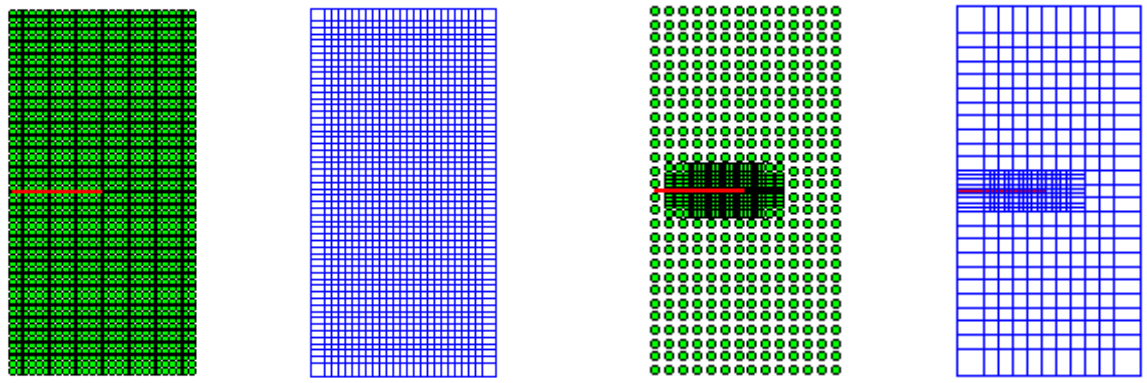


**Figure 5.** The used meshes of rectangular plate: (a) 1624 control points and (b) 1375 elements, for NURBS representation, (c) 566 control points and (d) 431 elements, for T-spline representation.

In Figure 6 and Table 1 the obtained SIFs are in good agreement with the other methods. T-splines provide a minimal number of nodes due to their ability in describing exactly such geometries. Also, the results of the edge crack problem (Figure 7) in both modes agree well for minimal number of degrees

of freedom compared to XFEM and NURBS based XIGA. The mode I SIF changes their trend in 45° and the mode II SIF changes their trend in 30°, so in orthotropic materials the stress intensity factors are not only depend on the crack angle, but they also depend on the direction of elasticity axes. For more details about the results that obtained by other numerical methods for this problem, the reader may refer to [23,69].

**Table 1.** Comparison of mixed mode stress intensity factors for a central inclined crack ($\beta$=30°) in orthotropic disk.

| Method | Number of nodes | Number of elements | Number of Degrees of freedom | $K_I$ | $K_{II}$ |
|---|---|---|---|---|---|
| MCC [7] | 2712 | 999 | 5424 | 16.73 | 11.33 |
| M-integral [69] | 2712 | 999 | 5424 | 16.75 | 11.38 |
| XEFG [23] | 877 | - | 1507 | 16.80 | 11.79 |
| NURBS based XIGA | 4489 | 4096 | 9266 | 16.70 | 11.38 |
| T-splines based XIGA | 793 | 688 | 1890 | 16.86 | 11.78 |

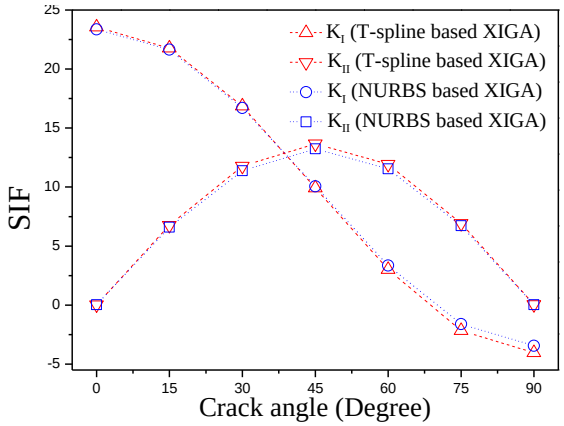


**Figure 6.** Variation of mode I and II SIFs with respect to different crack angles using analysis-suitable T-splines and NURBS for the circular plate.

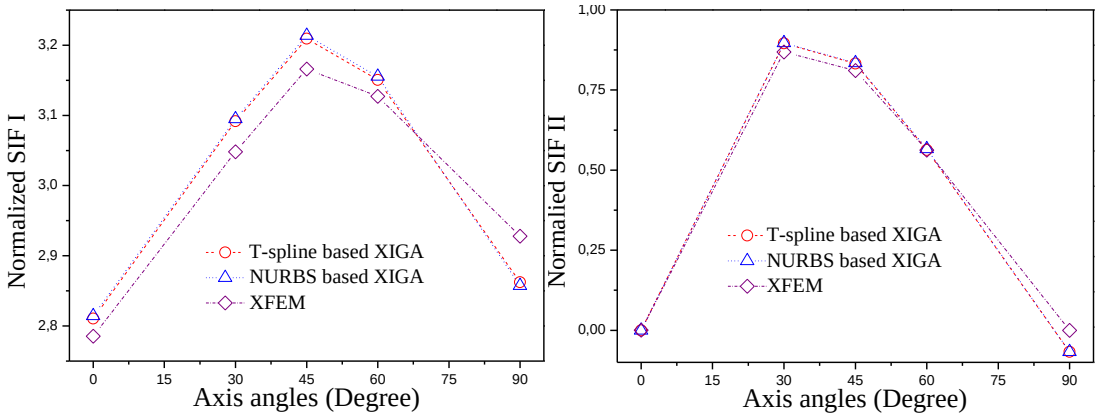


**Figure 7.** Variations of normalized mode I and II SIFs with respect to different angles of orthotropic axes using analysis-suitable T-splines, NURBS and XFEM for the rectangular plate.

## 7. Conclusion

Static fracture behaviour for a crack in orthotropic materials is analysed numerically in this study using the Extended Isogeometric Analysis (XIGA). NURBS and T-splines bases are used to define the exact geometry and approximate the solution throughout the analysis. Orthotropic crack-tip enrichment functions, which can be applied to all types of orthotropic materials, are implemented. SIFs for both mode I and II are evaluated using the M-integral to determine fracture properties of the domain. The quality of the obtained results regarding their good agreement with the results of literature demonstrates the accuracy of the present approach and the robustness of the developed code. The inclination angle of the orthotropic axes generates and affects the evolution of mixed mode SIF even if the crack is only subjected to mode I loading, therefore the mode II must also be evaluated.

## References

[1] Sih GC, Paris P and Irwin GR 1965 *International Journal of Fracture Mechanics* **1**(3) 189-203
[2] Bowie O and Freese C 1972 *International Journal of Fracture Mechanics* **8**(1) 49-57
[3] Kuo M and Bogy D 1974 *Journal of Applied Mechanics* **41**(1) 197-202
[4] Viola E, Piva A and Radi E 1989 *Engineering Fracture Mechanics* **34**(5) 1155-1174
[5] Hoenig A 1982 *Engineering Fracture Mechanics* **16**(3) 393-403
[6] Aliabadi M and Sollero P 1998 *Composites Science and Technology* **58**(10) 1697-1703
[7] Kim J-H and Paulino GH 2002 *Engineering Fracture Mechanics* **69**(14) 1557-1586
[8] Yue T and Abdel Wahab M 2014 *Wear* **321** 53-63
[9] Wang C, Sun Q, Abdel Wahab M, Zhang X and Xu L 2015 *Waste Management* **43** 19-27
[10] Yue T and Abdel Wahab M 2016 *Materials* **9**(7)
[11] Ferjaoui A, Yue T, Abdel Wahab M and Hojjati-Talemi R 2015 *International Journal of Fatigue* **73** 66-76
[12] Pereira K, Yue T and Abdel Wahab M 2017 *Tribology International* **110** 222-231
[13] Kumar D, Biswas R, Poh LH and Abdel Wahab M 2017 *Tribology International* **109** 124-132
[14] Bhatti NA and Abdel Wahab M 2017 *Tribology International* **109** 552-562
[15] Yue T and Abdel Wahab M 2016 *Materials* **9** 597; doi:510.3390/ma9070597
[16] Vanegas-Useche L, Abdel Wahab M and Parker G 2015 *Waste Management* **43** 28-36
[17] Resende Pereira KdF, Bordas S, Tomar S, Trobec R, Depolli M, Kosec G and Abdel Wahab M 2016 *Materials* **9** 639; doi:610.3390/ma9080639
[18] Noda N-A, Chen X, Sano Y, Wahab MA, Maruyama H, Fujisawa R and Takase Y 2016 *MATERIALS & DESIGN* **96** 476-489
[19] Junyan Ni and Wahab MA 2017 *Computers & Structures* **186** 35–49
[20] Yue T and Abdel Wahab M 2017 *Tribology International* **107** 274-282
[21] Martínez JC, Vanegas Useche LV and Wahab MA 2017 *International Journal of Fatigue* **100, Part 1** 32-49
[22] Ghorashi SS, Mohammadi S and Sabbagh-Yazdi S-R 2011 *Engineering Fracture Mechanics* **78**(9) 1906-1927
[23] Asadpoure A, Mohammadi S and Vafai A 2006 *Thin-Walled Structures* **44**(9) 1031-1038
[24] Asadpoure A, Mohammadi S and Vafai A 2006 *Finite Elements in Analysis and Design* **42**(13) 1165-1175
[25] Atluri SN, Kobayashi AS and Nakagaki M 1975 *International Journal of Fracture* **11**(2) 257-271
[26] Hughes TJ, Cottrell JA and Bazilevs Y 2005 *Computer Methods in Applied Mechanics and Engineering* **194**(39) 4135-4195
[27] X. Nguyen H, N. Nguyen T, Abdel Wahab M, Bordas SPA, Nguyen-Xuan H and P. Voa T 2017 *Computer Methods in Applied Mechanics and Engineering* **313** 904-940
[28] Tran Vinh L, Lee J, Nguyen-Van H, Nguyen-Xuan H and Abdel Wahab M 2015 *International Journal of Non-Linear Mechanics* **72** 42-52

[29] Tran LV, Phung-Van P, Lee J, Wahab MA and Nguyen-Xuan H 2016 *Composite Structures* **140** 655-667
[30] Thai CH, Ferreira AJM, Abdel Wahab M and Nguyen-Xuan H 2016 *Acta Mechanica* **227**(5) 1225-1250
[31] Thai C, Zenkour AM, Abdel Wahab M and Nguyen-Xuan H 2016 *Composite Structures* **139** 77-95
[32] Phung-Van P, Tran LV, Ferreira AJM, Nguyen-Xuan H and Abdel-Wahab M 2016 *Nonlinear Dynamics* 1-16; doi:10.1007/s11071-11016-13085-11076
[33] Phung Van P, Nguyen LB, Tran Vinh L, Dinh TD, Thai CH, Bordas SPA, Abdel Wahab M and Nguyen-Xuan H 2015 *International Journal of Non-Linear Mechanics* **76** 190-202
[34] Phung Van P, De Lorenzis L, Thai CH, Abdel Wahab M and Nguyen-Xuan H 2015 *Computational Materials Science* **96** 495-505
[35] Phung Van P, Abdel Wahab M, Liew KM, Bordas SPA and Nguyen-Xuan H 2015 *Composite Structures* **123** 137-149
[36] Cottrell JA, Reali A, Bazilevs Y and Hughes TJ 2006 *Computer Methods in Applied Mechanics and Engineering* **195**(41) 5257-5296
[37] Tran Vinh L, Lee J, Ly HA, Abdel Wahab M and Nguyen-Xuan H 2015 *International Journal of Mechanical Sciences* **96-97** 65-78
[38] Phung Van P, Tran Vinh L, Ferreira AJM, Nguyen-Xuan H and Abdel Wahab M 2016 *Nonlinear Dynamics* (http://dx.doi.org/10.1007/s11071-016-3085-6)
[39] Tran Vinh L, Phung Van P, Lee J, Abdel Wahab M and Nguyen-Xuan H 2016 *Composite Structures* **140** 655-667
[40] Thai C, Ferreira AJM, Abdel Wahab M and Nguyen-Xuan H 2016 *Acta Mech* **227**(5) 1225-1250
[41] Zhou Y-L, Maia N and Abdel Wahab M 2016 *Journal of Vibration and Control* doi: 10.1177/1077546316674544
[42] Zhou Y-L and Abdel Wahab M 2016 *Journal of Vibroengineering* **18**(7) 4491-4499
[43] Khatir S, Belaidi I, Serra R, Abdel Wahab M and Khatir T 2016 *Journal of Vibroengineering* **18**(1) 202-213
[44] Khatir S, Belaidi I, Serra R, Abdel Wahab M and Khatir T 2015 *Mechanika* **21**(6) 472-479
[45] Gillich G-R, Praisach Z-I, Abdel Wahab M, Gillich N, Mituletu IC and Nitescu C 2016 *Shock and Vibration* **2016**(Article ID 2086274) 10 pages; http://dx.doi.org/10.1155/2016/2086274
[46] Zhou Y-L, Maia NMM, Sampaio R and Wahab MA 2016 *Structural health monitoring* **DOI: https://doi.org/10.1177/1475921716680849**
[47] Temizer I, Wriggers P and Hughes T 2011 *Computer Methods in Applied Mechanics and Engineering* **200**(9) 1100-1112
[48] Willberg C and Gabbert U 2012 *Acta Mechanica* **223**(8) 1837-1850
[49] Bazilevs Y, Calo V, Zhang Y and Hughes TJ 2006 *Computational Mechanics* **38**(4-5) 310-322
[50] Buffa A, Sangalli G and Vázquez R 2010 *Computer Methods in Applied Mechanics and Engineering* **199**(17) 1143-1152
[51] Li K and Qian X 2011 *Computer-Aided Design* **43**(11) 1427-1437
[52] Irzal F, Remmers JJ, Verhoosel CV and Borst R 2014 *International Journal for Numerical Methods in Engineering* **97**(8) 608-628
[53] De Luycker E, Benson D, Belytschko T, Bazilevs Y and Hsu M 2011 *International Journal for Numerical Methods in Engineering* **87**(6) 541-565
[54] Bhardwaj G and Singh I 2015 *Journal of the Brazilian Society of Mechanical Sciences and Engineering* **37**(4) 1065-1082
[55] Nguyen-Thanh N, Valizadeh N, Nguyen M, Nguyen-Xuan H, Zhuang X, Areias P, Zi G, Bazilevs Y, De Lorenzis L, et al. 2015 *Computer Methods in Applied Mechanics and Engineering* **284** 265-291
[56] Peake MJ, Trevelyan J and Coates G 2013 *Computer Methods in Applied Mechanics and Engineering* **259** 93-102
[57] Bui TQ 2015 *Computer Methods in Applied Mechanics and Engineering* **295** 470-509

[58] Jia Y, Anitescu C, Ghorashi SS and Rabczuk T 2015 *IMA Journal of Applied Mathematics* **80**(3) 608-633
[59] Yu T, Bui TQ, Yin S, Doan DH, Wu C, Van Do T and Tanaka S 2016 *Composite Structures* **136** 684-695
[60] Guo Y, Ruess M and Gürdal Z 2014 *Composite Structures* **116** 55-66
[61] Ghorashi SS, Valizadeh N, Mohammadi S and Rabczuk T 2015 *Computers & Structures* **147** 138-146
[62] Sederberg TW, Zheng J, Bakenov A and Nasri A 2003 ACM transactions on graphics (TOG) ed editors) ACM p. 477-484
[63] Li X, Zheng J, Sederberg TW, Hughes TJ and Scott MA 2012 *Computer Aided Geometric Design* **29**(1) 63-76
[64] Scott M, Li X, Sederberg T and Hughes T 2012 *Computer Methods in Applied Mechanics and Engineering* **213** 206-222
[65] Asadpoure A and Mohammadi S 2007 *International Journal for Numerical Methods in Engineering* **69**(10) 2150-2172
[66] Shojaee S, Asgharzadeh M and Haeri A 2014 *International Journal of Applied Mechanics* **06**(06) 1450068
[67] Shojaee S and Daneshmand A 2015 *Engineering Fracture Mechanics* **147** 203-227
[68] Kim J-H and Paulino GH 2003 *International Journal of Solids and Structures* **40**(15) 3967-4001
[69] Lekhnitskii S 1963 Of an anisotropic elastic body ed editors. San Francisco: Holden-Day